Polymer Testing 152 (2025) 108974

Contents lists available at ScienceDirect

Polymer Testing

journal homepage: www.elsevier.com/locate/polytest

Round-robin programme for longitudinal tensile testing of unidirectional composites: results, conclusions, and recommendations

Babak Fazlali [a], Christian Breite [a], Gergely Czél [b,c,*], Bodo Fiedler [d], Dennis Gibhardt [d], Masaki Hojo [e], Hannes Koerber [f], Rajnish Kumar [g], María Luisa Velasco [h], Ian McEnteggart [i], Lars P. Mikkelsen [g], Federico Paris [h], Ichiro Taketa [j], Michael R. Wisnom [k], Yentl Swolfs [a]

[a] Department of Materials Engineering, KU Leuven, Kasteelpark Arenberg 44 box 2450, 3001, Leuven, Belgium
[b] Department of Polymer Engineering, Faculty of Mechanical Engineering, Budapest University of Technology and Economics, Műegyetem rkp. 3, H-1111, Budapest, Hungary
[c] MTA-BME Lendület Sustainable Polymers Research Group, Budapest University of Technology and Economics, Műegyetem rkp. 3, H-1111, Budapest, Hungary
[d] Institute of Polymers and Composites, Hamburg University of Technology, Denickestraße 15, 21073, Hamburg, Germany
[e] Kyoto University, Kinki Polytechnic College, 3-1-1, Kishinooka-cho, Kishiwada, Osaka, 596-0817, Japan
[f] ZwickRoell GmbH & Co. KG, August-Nagel-Straße 11, 89079, Ulm, Germany
[g] Department of Wind and Energy Systems, Technical University of Denmark, Frederiksborgvej 399, 4000, Roskilde, Denmark
[h] Department of Continuum Mechanics and Theory of Structures, Universidad de Sevilla, Camino Descubrimientos, s/n Isla Cartuja, 41092, Sevilla, Spain
[i] Instron, Coronation Road, High Wycombe, HP12 3SY, United Kingdom
[j] Toray Industries, Inc., 1515, Oaza Tsutsui, Masaki-cho, Iyo-gun, Ehime, 791-3193, Japan
[k] Bristol Composites Institute, University of Bristol, Queen's Building, University Walk, BS8 1TR, Bristol, United Kingdom

ARTICLE INFO

Keywords:
Tensile testing
Unidirectional composites
Polymer-matrix composites
Carbon fibre composites

ABSTRACT

The longitudinal tensile behaviour is one of the most important and basic characteristics of a unidirectional composite, yet its experimental characterisation is not straightforward. Therefore, we conducted a round-robin programme with seven test labs and six coupon designs where the panels were manufactured and cut by the same lab. Our results indicate that careful manufacturing and cutting enable consistent and reliable results for the different labs and coupon designs. High-speed videos confirmed that many coupons failed away from the grips, which is the targeted failure location. In addition to the modulus, failure strain and strength results, we present results and novel recommendations related to the coupon preparation and testing methodology. We recommend using a non-contact strain measurement method and discarding tests with significant stress drops before final failure.

1. Introduction

The tensile strength of multidirectional laminates is underpinned by the longitudinal tensile strength of the unidirectional plies, and a direct relation between the two was demonstrated if premature failure due to delamination is avoided [1]. Therefore, accurate methods for measuring longitudinal tensile strength are vital to help establish the potential laminate strength that could be attained in realistic multidirectional laminates. Longitudinal tensile strength is often characterised in industry and academia, as it serves as the basis for laminate design, material selection, and simulations.

ASTM and ISO standards for tensile testing of composites have been widely adopted in the field, and they are rather similar. The ASTM D3039 standard [2] covers tensile testing of composites and allows minor variations in the recommended dimensions for unidirectional composites. The ISO 527 standard [3] has a specific substandard 527–5 [4] for unidirectional composite coupons, but this standard proposes only minor modifications compared to multidirectional ones.

In the last two decades, it has become clear that longitudinal tensile testing of unidirectional composites has some challenges that the standards cover insufficiently [5]. Firstly, stress concentrations are more severe and extend over a larger distance than in multidirectional composites [6]. Combined with a greater sensitivity to stress concentrations, achieving acceptable failure is challenging [7–9]. Secondly, although

* Corresponding author. Department of Polymer Engineering, Faculty of Mechanical Engineering, Budapest University of Technology and Economics, Műegyetem rkp. 3, H-1111, Budapest, Hungary.
E-mail addresses: czel.gergely@gpk.bme.hu (G. Czél), yentl.swolfs@kuleuven.be (Y. Swolfs).

https://doi.org/10.1016/j.polymertesting.2025.108974
Received 27 June 2025; Received in revised form 25 August 2025; Accepted 5 September 2025
Available online 5 September 2025

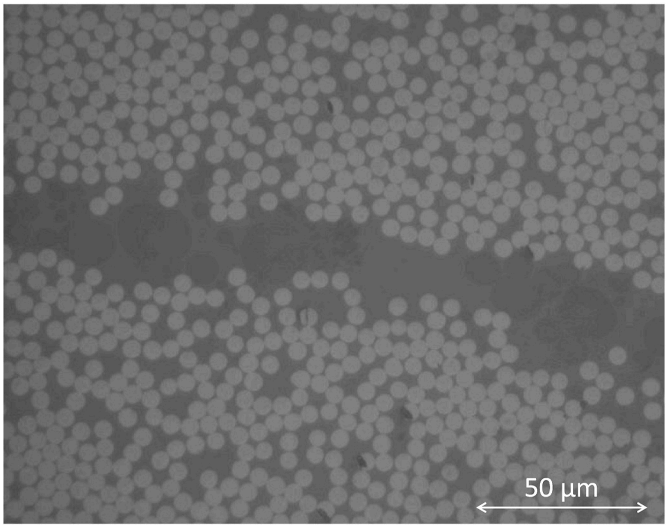

Fig. 1. Optical microscopy image at a ply interface, showing a near void-free composite.

the ASTM standard mandates failure in the gauge section, this is difficult to verify in practice [5,10,11]. Unidirectional composites tested in longitudinal tension fail so rapidly and explosively that the initial failure location is challenging to detect. A high-speed camera would be required to identify this location [12], but this is rarely done. Thirdly, several recent reports have demonstrated that alternative coupon designs may be more effective in mitigating stress concentrations and triggering failure within the gauge section than the standardised coupon designs [13,14].

We note a few recent developments in coupon designs that have shown significant potential compared to the standardised end tabs, which are either rectangular or tapered. Czél et al. [13] introduced the sandwich design to eliminate the stress concentrations within the laminate to be tested. This design creates fibre-hybrid composites with the investigated material in the middle and layers of a material with a higher failure strain on the outside. Typically, this implies unidirectional carbon fibre composite layers sandwiched between glass fibre composite layers. While longitudinal stress concentrations persist in the glass fibre composite layers, modelling results confirmed that they can be eliminated in the carbon fibre composite layers [13]. A later study [14] showed that the glass fibre composite layer should have at least the same thickness as the central carbon fibre composite layer to eliminate the stress concentration for the investigated material combination. However, strong reductions in stress concentrations are already present even for thinner glass fibre composite layers [14]. The sandwich design can provide failure strain results directly, but stress back-calculation is required to obtain tensile strength values, introducing new uncertainties. A minor drawback is that residual stress correction is required if the plies are co-cured at elevated temperatures [15]. These stresses can be avoided by bonding the layers with an adhesive that cures at room temperature [16,17]. Additional considerations are necessary regarding resin compatibility between both ply types. Furthermore, if surface roughening is required to achieve good bonding, this may potentially harm the fibres.

Another approach to removing stress concentrations from the gauge section is to gradually taper the width, leading to a design often called butterfly coupons [18,19]. In contrast with dogbone coupons [20], these coupons have a very large radius of curvature, which can help to delay splitting along this radius as much as possible. Kumar et al. [16] showed that butterfly coupons with a 0.9 m radius of curvature increased the measured failure strain by 8.4 % compared to conventional rectangular coupons. Further increasing the radius of curvature to 3.75 m led to X-butterfly coupons, which increased the measured failure strain by 9.9 % compared to rectangular coupons. Another key advantage of the (X-)butterfly design is that it increases the gripping area relative to the central cross-sectional area. This area is particularly important for thicker coupons, where the high required gripping force can cause failure in the gripped section. Korkiakoski et al. [18] showed substantial benefits of the butterfly design regarding fatigue life, whereas more recent work showed the opposite [21]. Further improvements were achieved when the sandwich design was combined with the butterfly design [16], which indicates that the full potential was not yet achieved. Another study on thin coupons [14] revealed that rectangular sandwich coupons resulted in higher failure strains than butterfly coupons. These discrepancies for thin coupons are likely due to differences in the cutting quality, which may trigger premature splitting and failure to a different extent depending on the coupon design. This splitting is the main challenge of this design, even with very large radii of curvature.

Several authors have proposed tabs that are not rectangular but oblique [22,23]. Such tabs introduce the stress concentrations more gradually. Oblique tabs are common in testing unidirectional composites in an off-axis direction. In the fibre direction, such an approach is rare because it introduces significant asymmetry. Therefore, Fazlali et al. [14] proposed arrow-shaped end tabs to gradually introduce the stress into the coupon while maintaining symmetry. Their results revealed that arrow-tabbed and sandwich designs achieved the highest failure strain and that butterfly, tapered- and rectangular-tabbed designs underperformed.

Instead of tapering the end tabs, it is also possible to taper the thickness of the composite via ply drops or machining. This approach achieved consistent failure within the gauge section [24,25] and increased the measured strength by 13.7 % compared to conventional specimens [10]. The tape-scarfing design follows a similar concept but cuts the ply ends at an angle [26]. This design avoids the need for end tabs and creates a more gentle transition than the traditional perpendicular cutting method, thus reducing stress concentrations and helping delay or avoid delamination at the ply drop [27]. Four-point bending tests on sandwich beams are another noteworthy strategy. This method is standardised for characterising compression strength [28] but can also be used for tensile strength with some modifications. The stress variation over the cross-section of the investigated composite can be minimised by making the core sufficiently thick and the skins sufficiently thin. Using a thicker skin on the compression than on the tensile side can guarantee failure on the tensile side. This strategy requires some optimisation regarding dimensions, core material and adhesive selection. Its main drawback lies in having a smaller volume under high stress than in usual coupon sizes, which may increase strength owing to size scaling effects.

A holistic and objective comparison of the different designs is currently missing. In addition, the published studies also have significant differences in procedures, such as coupon preparation, grip and coupon alignment, and strain measurement methods. There is room for improving the current standards and testing procedures for the longitudinal tensile testing of unidirectional composites. The field would benefit significantly from a standard that is tuned specifically to this case. We, therefore, set up a round-robin programme to compare seven different labs and six different coupon designs. This paper presents the results and main conclusions from this round-robin programme and provides all the data behind it as a Zenodo dataset [29].

2. Materials and methods

2.1. Materials and manufacturing

Toray Industries, Inc. (Ehime, Japan) manufactured all panels from T800S carbon fibres in a 3900-2B epoxy resin. This is an interlayer toughened prepreg commonly used in aerospace. The plies had a fibre areal density of 192 g/m^2 and a fibre weight fraction of 64.5 %, corresponding to a fibre volume fraction of about 55 %. Five and 25 plies, respectively, were laid up by hand to create laminates with nominal

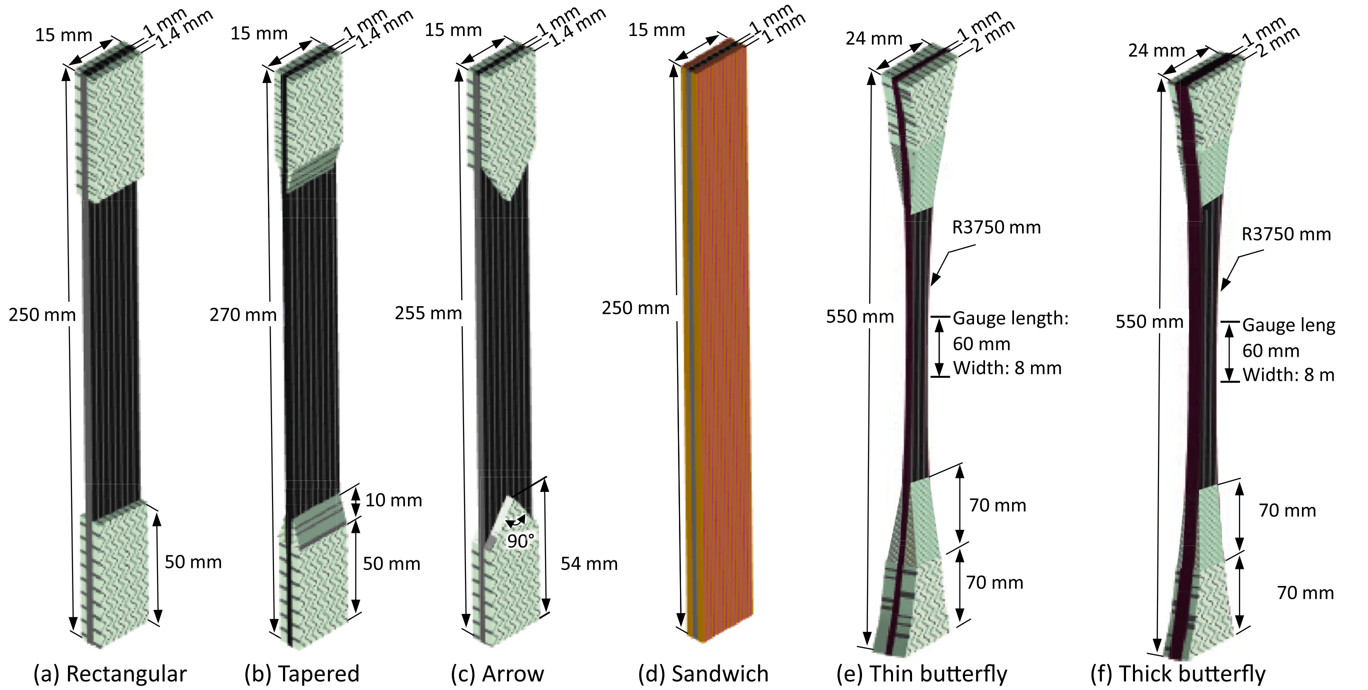

Fig. 2. Overview of the six coupon designs. Note that the scale of (a–d) differs from the one of (e,f).

thicknesses of 1 mm and 5 mm. These laminates were cured in an autoclave according to the manufacturer's recommendations: 1.7 °C/min ramp to 180 °C followed by a dwell for 2 h at 7 bar of pressure. This led to high-quality composites that are nearly void-free (see Fig. 1). Two distinct specimens were scanned using computed tomography and the structure tensor method, implemented in VoxTex [30], was used to analyse their fibre alignment. This resulted in standard deviations of 2.5–2.7° for the in-plane and out-of-plane misalignments. One edge along the 90° direction was cut directly after curing to serve as a reference edge for aligning the rest of the cutting procedures.

In addition, Toray manufactured panels to serve as end tab material. These were made of balanced, 8-harness satin, glass fibre weaves aligned in the ±45° direction, leading to a panel thickness of 1.4 mm. The five plies were offset by 2.5 mm each time for the tapered tabs to create a taper with an 8° angle. The tab panels were bonded to the already cured carbon fibre laminates using AF126 adhesive film from 3M (St. Paul, USA). This assembly was cured in an autoclave at 120 °C. There are three exceptions. Firstly, the arrow tabs were water jet cut from the panels. These individual tabs were then bonded to individual coupons using Araldite 2011 adhesive from Huntsman (Basel, Switzerland) and cured at 95 °C. Secondly, the sandwich coupons did not use any end tabs. Instead, 1 mm thick protective plates made of four S-glass fibre plies were bonded to each side of the cured carbon fibre laminate using the same Araldite 2011 adhesive as explained in detail in Ref. [17]. In this case, however, the adhesive was cured at room temperature to eliminate thermal residual strains. A distributed force of approximately 400 N was applied on the 300 × 300 mm sandwich plates during curing. The S-glass/913 epoxy plies were supplied by Hexcel and had a fibre areal density of 305 g/m^2 and fibre volume fraction of 50 %. Thirdly, the butterfly coupons used a biaxial glass fibre composite laminate from Electro-Isola A/S (Vejle, Denmark) with a thickness of 2 mm and oriented at ±45°. These tabs were bonded before machining using a DP460 structural adhesive from 3M (St. Paul, USA), which was cured for 24 h at room temperature and 16 h at 40 °C.

2.2. Coupon preparation

We have assessed six possible unidirectional coupon designs, which we will refer to as rectangular, tapered, arrow, sandwich, thin butterfly and thick butterfly. Rectangular and tapered are the two coupon designs recommended by the ASTM D3039 standard, whereas the ISO 527 standard only recommends rectangular tabs. For the butterfly design, we tested the unidirectional composites with a nominal thickness of 1 mm and the thicker ones of 5 mm. These two are referred to as "thin butterfly" and "thick butterfly", respectively. Their full terminology in recent publications would be X-butterfly [16,31]. Fig. 2 provides the full dimensions of all the coupon designs. Note that the thin butterfly coupon has a smaller gauge volume than the first four coupon designs. However, Kumar et al. [31] suggested that the expected strength reduction from the smaller volume is limited to 1–2 %, and this was for a design with a radius of curvature of 900 mm (instead of the 3750 mm we used).

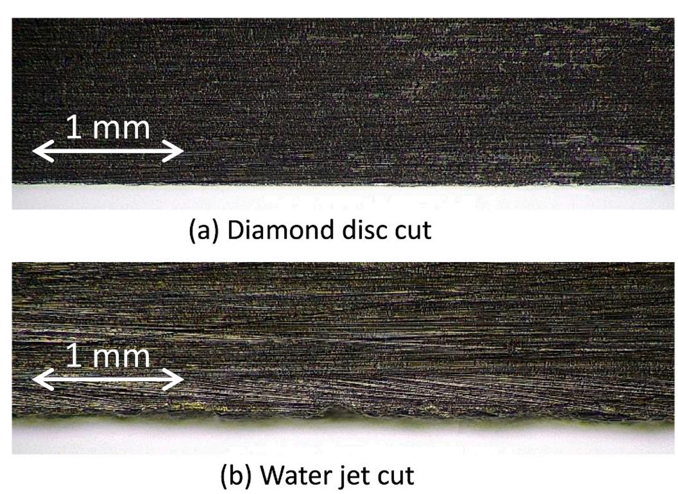

Fig. 3. Comparison of cut quality between (a) diamond disc and (b) water jet.

During initial trials, we attempted to achieve a high cutting quality via water jet cutting because this enables us to use a consistent cutting method for all coupon designs. The main parameters controlling the quality of the water jet cut that we attempted to optimise are the nozzle diameter, the pressure, the thickness, and the type of protective layer used on top of the plate.

Fig. 3 compares the quality of diamond disc and water jet cutting. The quality of the cut achieved with diamond disc is relatively smooth, while the water jet produces a rougher, more jagged edge. As demonstrated in section 3.2, the water jet cut did not yield satisfactory results, even after several iterations. We, therefore, switched to diamond disc cutting for all coupons apart from the butterfly ones, which were machined. A fine diamond disc with grade 181 and a thickness of 1 mm was used. The butterfly coupons were milled using a computer-numerical controlled machine (Qtec Automation and Waterjet Technology Aps, Denmark) equipped with a 6 mm diameter carbide cutting tool. Parameters such as the rotation and feed rate were systematically adjusted considering the thickness of the coupon to achieve an optimal edge quality.

The coupons from different panels were randomised before they were sent out to the participants. This ensured all participants had coupons from various panels and random locations within the panel. The origin of the individual coupons was still tracked so we could perform a meta-analysis based on all the received results.

2.3. Tensile testing methodology

Table 1 summarises the testing methodology used by the seven different labs. These labs include Budapest University of Technology and Economics, Hamburg University of Technology, Instron, KU Leuven, Technical University of Denmark, University of Seville, and ZwickRoell. These labs are randomly ordered and anonymised in Table 1 and the rest of this paper. Two labs used both hydraulic and mechanical grips on some designs, which will be indicated by “hydr.” and “mech.”, respectively.

All labs used wedge-acting grips with a moving body and stationary wedges. Some participants used two strain measurement methods. In such cases, we have only used the optical extensometer data for the reasons described in section 3.3. All participants were requested to target a strain rate of 1 %/min. However, universal testing machines are displacement-driven and often do not have a direct feedback loop for strain measured on the coupon itself. We, therefore, recommended strain rates in the range of 0.5–2 %/min, for which we do not expect any measurable strain rate sensitivity [32,33].

We recommended an overhang distance of 3 mm, meaning the flat section of the grips extends over the end tabs by 3 mm (see Fig. 4a and b). For the arrow design, the tip sticks out of the grips by 1.5 mm (see Fig. 4c). For the sandwich designs, Mirka Abrasive Yellow Basic sandpaper of grit size P80 was recommended and provided with an approximate overhang of 5 mm from the grips. All other designs had conventional end tabs and did not require sandpaper. Nevertheless, Lab 5 was the only lab to still use sandpaper on these other designs.

2.4. Data reduction

The individual labs performed the basic data treatment and shared all their stress-strain data with KU Leuven. KU Leuven then ensured that the strains were shifted to the origin so that the fitted trendline between strains of 0.1 % and 0.3 % extrapolates through the origin. Section 3.4 presents a further analysis of the effect of this method.

Some stress-strain datasets were missing reliable strain data in the last 0.1–0.2 % strain regime. Such datasets were ignored for failure strain but still used for modulus and strength evaluation. This issue arises mainly because splitting or surface damage caused issues with strain registration, which happened for all labs but was more frequent for labs using strain gauges. All the extracted parameters were verified for outliers. The values were discarded if the data point was more than three standard deviations from the mean (not considering the data point

Table 1
Overview of the testing methodology at the seven different labs.

Lab	1	2	3	4	5	6	7
Thickness measurement	Digital micrometre screw gauge (flat tip, Ø6.35 mm)	Digital micrometre screw gauge (flat tip, Ø6.35 mm)	Digital height gauge (supported over a length of 95 mm, ball tip, Ø3 mm)	Digital micrometre screw gauge (flat tip, Ø6.35 mm)	Digital micrometre screw gauge (flat tip, Ø6.35 mm)	Digital micrometre screw gauge (flat tip, Ø6.35 mm)	Digital micrometre screw gauge (flat tip, Ø6.35 mm)
Width measurement	Digital calliper	Digital calliper	Digital calliper	Digital micrometre screw gauge	Digital micrometre screw gauge	Digital calliper	Digital calliper
Strain measurement method	Full-field DIC, 90 mm gauge length	Optical extensometer, 50 mm gauge length (used) and strain gauge 6 mm gauge length (not used)[b]	Two strain gauges averaged together, 6 mm gauge length	One strain gauge, 6.25 mm gauge length	Mechanical extensometer, 50 mm gauge length	Optical extensometer, 50 mm gauge length	Optical extensometer (used) and mechanical extensometer (not used)[b], both 50 mm gauge length
Test machine frame capacity (kN)	250	250	100 and 250	150 (mechanical) and 250 (hydraulic)	400 (mechanical) and 100 (hydraulic)	250	300
Load cell capacity (kN)	250	250	100 and 250	150 (mechanical) and 250 (hydraulic)	400 (mechanical) and 100 (hydraulic)	250	300
Grip type/ capacity (kN)	Hydraulic/100	Mechanical/100	Hydraulic/100[a]/250	Hydraulic/250 and mechanical/150	Hydraulic/100 and mechanical/100	Hydraulic/250	Hydraulic/300
Grip alignment	Full correction in all directions	Manual alignment	Full correction in all directions	Full correction in all directions	Correction in some directions	Full correction in all directions	Full correction in all directions
Coupon alignment	L-shaped profile	Marks on grip faces + based on video feed	Based on the video feed	Centre points of coupon and grips	L-shaped profile	Stops mounted on grips + alignment in video feed	Stops mounted on grips
Coupon conditioning	Ambient conditions of 25 °C and 50 %RH	Ambient conditions of 25 °C and 40–50 %RH	Preconditioned at least 24 h at 21.7 °C and 59 % RH	Preconditioned for 2 months at 24–25 °C and 50–55 % RH	Preconditioned for 2 weeks at 21–23 °C and 50–59 % RH	Ambient conditions of 21–23 °C and 45–50 %RH for 2 months	Ambient conditions of 20–22 °C and 40–50 %RH
Test temperature (°C)	23	25	21.9–22.1	21–25	21–22	22.9–23.9	21–22

[a] 5 of the sandwich coupons were tested using a grip with a capacity of 100 kN. All others were tested using a grip with a 250 kN capacity.
[b] (not used) indicate that this measurement method has not been used in the data analysis of the measurements.

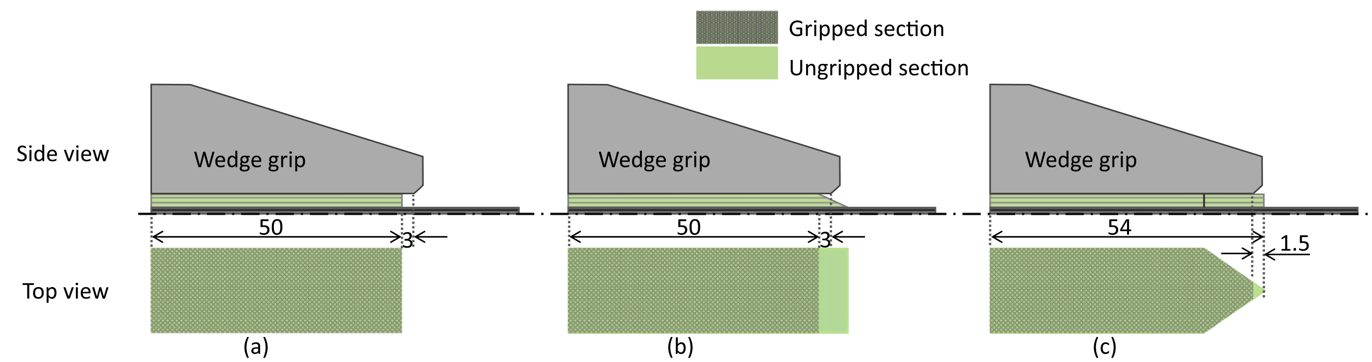

Fig. 4. Position of the end tabs relative to the grips: (a) rectangular tabs, (b) tapered tabs, and (c) arrow tabs.

itself).

KU Leuven performed the required stress back-calculation for all the sandwich coupons. The back-calculated stress $\sigma^{i}_{CF,sandwich}$ in the carbon fibre layers of sandwich coupon i was obtained based on Eq. (1):

$$\sigma^{i}_{CF,sandwich}(\varepsilon) = \sigma^{i}_{sandwich}(\varepsilon) . \frac{E^{avg}_{CF,rect}(\varepsilon)}{E^{i}_{sandwich}(\varepsilon)} \tag{1}$$

where $E^{avg}_{CF,rect}$ is the average tangent modulus of all fitted second-order polynomials through the rectangular coupon data of that specific lab and $E^{i}_{sandwich}$ is the tangent modulus based on the fitted second-order polynomial for the particular sandwich coupon i. We used a second-order polynomial fit because previous research has established that this is a good representation of the nonlinear elasticity of carbon fibre composites [16]. The diagrams were always fitted until 1.5 % strain unless a significant stress drop was found before that strain level, in which case only data points before that point were considered. The 1.5 % threshold was chosen because the stress-strain data was smooth up until this point for most diagrams. However, in a few cases, the fit was stopped a bit earlier.

We evaluated the modulus as the slope of the fitted trendline in the 0.1–0.3 % strain region. We used the maximum stress based on individually measured coupon cross-sectional areas as the tensile strength and the corresponding strain as the failure strain. Section 3.4 proposes and analyses an alternative definition. The cross-sectional areas were measured in three locations along the length, all of which yielded very consistent values.

3. Results and discussion

Tensile tests on unidirectional composites can be affected by different parameters. We will first investigate the effect of coupon design before zooming in on cutting, testing methodology and data reduction methodology.

3.1. Coupon design

Fig. 5 shows example stress-strain diagrams from arrow and sandwich coupons tested by one lab. The diagrams for arrow coupons (see Fig. 5a) nearly overlap until a strain of 1.7 %, confirming excellent coupon-to-coupon consistency. Some minor stress drops of 100 MPa or less start appearing at 1.7 % strain in most diagrams. These drops indicate that premature damage, like splitting along the specimen edge, was almost but not entirely avoided. For some coupon designs or labs, these premature load drops were a bit larger or started occurring at earlier strains. For sandwich coupons (see Fig. 5b), these drops tended to be small or absent.

Table 2 summarises all modulus, strength and failure strain results, and Fig. 6 visually represents the modulus results. While the lab-to-lab variations are larger than the design-to-design variations, they do remain small overall. The coefficients of variation fluctuate from 0.9 % to 4.3 %, with 77 % of the coefficients being below 2.5 % (see Table 2). These are reasonably low values, indicating good accuracy in the strain and load readings at low load levels. Labs 4 and 5 measured significantly

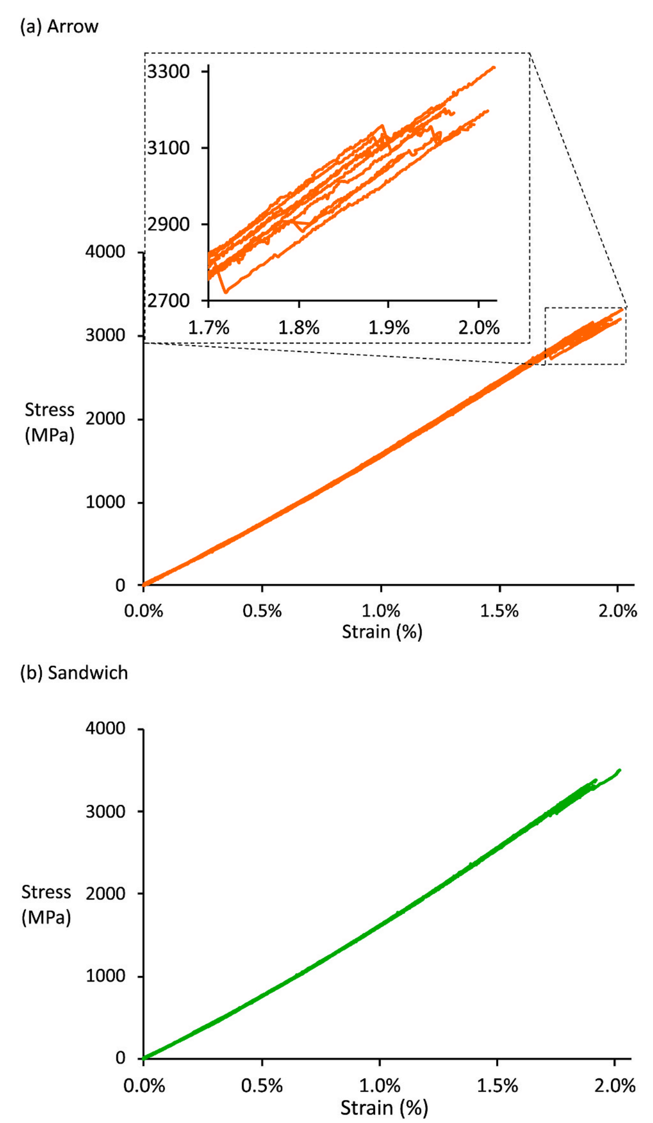

Fig. 5. Stress-strain diagrams of (a) all ten tests on arrow coupons and (b) all twelve tests on sandwich coupons from Lab 1. Additional stress-strain curves can be found in Zenodo dataset [29].

Table 2
Overview of all the mean values and their 95 % confidence interval for tensile modulus, strength and failure strain. The numbers between brackets indicate the coefficient of variation.

	Lab 1	Lab 2	Lab 3	Lab 4-hydr.	Lab 4-mech.	Lab 5-hydr.	Lab 5-mech.	Lab 6	Lab 7
					Modulus (GPa)				
Rectangular	146 ± 3 (2.4 %)	147 ± 2 (1.5 %)	146 ± 1 (0.9 %)	151 ± 1 (1.2 %)	150 ± 1 (1.0 %)	–	–	143 ± 2 (1.5 %)	145 ± 2 (2.0 %)
Tapered	145 ± 2 (2.2 %)	146 ± 1 (1.1 %)	–	153 ± 1 (1.3 %)	153 ± 1 (1.2 %)	151 ± 3 (2.9 %)	–	145 ± 1 (1.0 %)	147 ± 3 (2.6 %)
Arrow	147 ± 2 (1.8 %)	146 ± 1 (1.2 %)	147 ± 1 (0.9 %)	–	153 ± 1 (0.8 %)	152 ± 4 (3.9 %)	–	143 ± 2 (1.5 %)	146 ± 2 (2.3 %)
Sandwich	64 ± 1 (1.8 %)	63 ± 1 (1.4 %)	65 ± 1 (1.7 %)	–	67 ± 1 (1.8 %)	65 ± 1 (2.5 %)	–	64 ± 1 (1.9 %)	65 ± 2 (3.4 %)
Thin butterfly	149 ± 4 (3.1 %)	147 ± 1 (1.2 %)	145 ± 1 (1.3 %)	149 ± 2 (1.6 %)	150 ± 4 (3.3 %)	144 ± 4 (3.8 %)	–	145 ± 1 (1.1 %)	148 ± 5 (4.3 %)
Thick butterfly	–	–	147 ± 1 (0.8 %)	–	–	–	–	145 ± 1 (1.1 %)	147 ± 4 (3.8 %)
					Strength (MPa)				
Rectangular	3072 ± 143 (6.0 %)	3016 ± 121 (5.6 %)	3124 ± 57 (2.5 %)	3061 ± 92 (4.2 %)	3110 ± 79 (3.5 %)	3083 ± 116 (5.3 %)	3030 ± 93 (3.7 %)	3068 ± 141 (6.4 %)	3114 ± 97 (4.4 %)
Tapered	2940 ± 146 (6.9 %)	3006 ± 125 (6.2 %)	–	3095 ± 90 (3.8 %)	3124 ± 82 (3.1 %)	3065 ± 132 (5.6 %)	3013 ± 170 (7.3 %)	3039 ± 136 (6.7 %)	3099 ± 87 (4.2 %)
Arrow	3178 ± 46 (2.0 %)	3134 ± 39 (1.7 %)	3155 ± 61 (2.5 %)	–	3120 ± 47 (2.1 %)	3153 ± 69 (3.0 %)	–	3155 ± 65 (2.9 %)	3178 ± 56 (2.5 %)
Sandwich	3257 ± 67 (3.3 %)	3375 ± 60 (2.5 %)	–	–	3472 ± 71 (2.6 %)	3222 ± 158 (6.9 %)	–	3222 ± 90 (3.9 %)	3272 ± 102 (4.4 %)
Thin butterfly	3108 ± 99 (3.8 %)	3086 ± 66 (3.0 %)	3100 ± 36 (1.5 %)	3085 ± 96 (4.3 %)	3092 ± 96 (4.1 %)	3115 ± 80 (3.6 %)	–	3118 ± 67 (2.8 %)	3200 ± 51 (2.2 %)
Thick butterfly	–	–	2796 ± 43 (2.1 %)	–	2843 ± 46 (2.3 %)	–	–	2852 ± 59 (2.7 %)	2808 ± 92 (4.6 %)
					Failure strain (%)				
Rectangular	1.92 ± 0.05 (3.3 %)	1.91 ± 0.05 (3.4 %)	1.95 ± 0.03 (1.9 %)	–	1.89 ± 0.05 (3.2 %)	–	–	1.93 ± 0.07 (5.1 %)	1.93 ± 0.04 (2.6 %)
Tapered	1.88 ± 0.04 (3.0 %)	1.87 ± 0.06 (4.5 %)	–	–	1.89 ± 0.07 (3.7 %)	–	–	1.92 ± 0.04 (3.2 %)	1.91 ± 0.05 (3.7 %)
Arrow	1.96 ± 0.02 (1.8 %)	1.93 ± 0.02 (1.3 %)	1.97 ± 0.03 (2.0 %)	–	1.87 ± 0.03 (2.3 %)	1.82 ± 0.06 (3.1 %)	–	1.99 ± 0.04 (2.5 %)	1.96 ± 0.02 (1.5 %)
Sandwich	1.86 ± 0.04 (3.3 %)	1.97 ± 0.03 (2.2 %)	–	–	1.94 ± 0.03 (2.1 %)	–	–	1.88 ± 0.05 (3.5 %)	1.93 ± 0.03 (2.0 %)
Thin butterfly	1.90 ± 0.05 (3.0 %)	1.91 ± 0.04 (2.3 %)	1.91 ± 0.02 (1.3 %)	–	1.88 ± 0.04 (2.7 %)	1.88 ± 0.02 (1.1 %)	–	1.91 ± 0.04 (3.0 %)	1.95 ± 0.04 (2.0 %)
Thick butterfly	–	–	1.71 ± 0.02 (2.0 %)	–	–	–	–	1.76 ± 0.04 (3.1 %)	1.71 ± 0.05 (3.2 %)

higher modulus values: 149–151 GPa on average versus 144–147 GPa for the other labs. We did not identify a clear reason for this 3–5 % discrepancy. We do remark that load cells are typically considered good when they are within ±0.5 % of the calibration, which already explains a small part of this scatter.

Fig. 7 summarises the measured strength and failure strain values. The highest strength is measured for the sandwich coupons (see Fig. 7c), but its failure strain (see Fig. 7d) is not higher than that of the other coupons. We believe that this is due to the sandwich coupons suppressing edge splitting, which is evident in the stress-strain diagrams: they tend to have no load drops until the end (see Fig. 5b), whereas small load drops are reasonably common in all other coupon designs (see Fig. 5a). This indicates that this design is an effective method of suppressing early damage initiation. Sandwich coupons seem to be a reliable way to measure the failure strain, but the conclusion on their strength is less obvious. They did yield a higher strength than the other designs, but the exact figures may be affected by inaccuracies in the required stress back-calculation. However, no major discrepancies are expected since the back-calculated stress values are based on the individual stress-strain curves of the sandwich coupons, only taking a modulus factor into account based on the very consistent data of the rectangular coupon series.

The average strength reported in Fig. 7a varies from 2796 to 3472 MPa, with a global average of 3096 MPa. The average strength of the thick butterfly coupons (2824 MPa) is significantly lower than that of the other designs. This was expected because these coupons have a larger tested volume: assuming a Weibull modulus of 30–50 for the composite, we would expect a five-fold increase in volume (relative to the thin butterfly coupons) to reduce the strength by 3–5.5 %. That would explain about half of the observed difference. The other half is likely explained by the higher required failure load, which makes them intrinsically more difficult to test accurately due to the higher loads that need to be introduced at the grips. In addition, these coupons also seem to be more prone to splitting, which may be due to difficulties in achieving the same cutting quality as for thin coupons. The thick butterfly design is particularly relevant for thick composites, which (1) are difficult to test properly owing to the high gripping forces required and (2) are ignored by the current standards despite being important in some industries.

Ignoring the sandwich coupons, the arrow design yielded the highest strength, which was statistically significant relative to the thin butterfly design, with a p-value of 0.9 %. With a coefficient of variation of 2.4 % over all the labs, the arrow design also yielded the lowest scatter on the strength values and the highest failure strain (see Fig. 7d). The failure strain values of the thin coupons (rectangular, tapered, arrow, sandwich, and thin butterfly) are statistically significantly higher than for the thick butterfly coupons. However, among these thin coupons, there are no statistically significant differences.

Overall, the differences between the labs and the designs are all smaller than expected. This finding confirms that achieving consistent and reliable tensile test data for unidirectional composites is possible

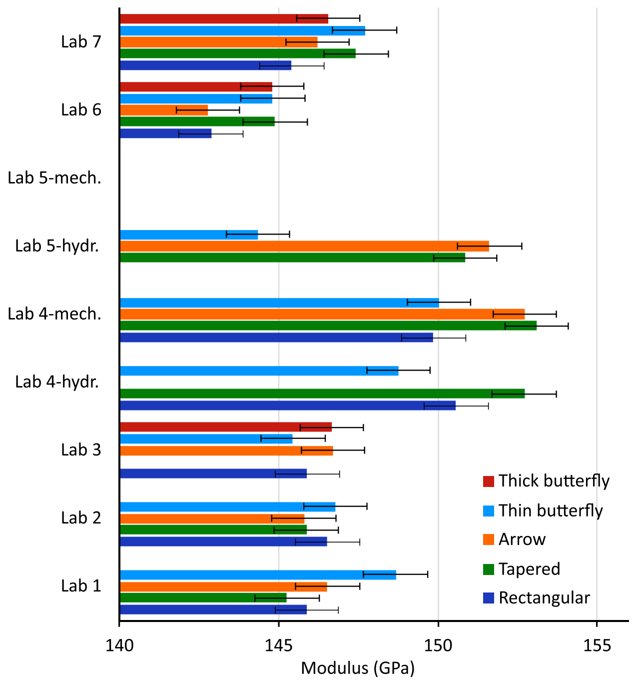

Fig. 6. The average measured moduli and their 95 % confidence intervals for the different labs and coupon designs.

with careful coupon preparation, testing procedures, and data reduction. This is possible even with the standardised coupon designs: rectangular and tapered.

Failure observations were requested from all labs, but this was very difficult in practice. The unidirectional composites often fail multiple times along their length owing to the compressive shockwave created when the elastic energy was released upon tensile failure. The coupons are shattered into many pieces after the test, making it difficult to detect the fracture location. There were, however, two exceptions to these difficulties. Firstly, the failure location was relatively easy to detect in the sandwich coupons because the glass fibre laminates held together the fractured carbon fibre laminate. Therefore, several labs reported that most sandwich coupons failed away from the grips. The fact that not all of them failed away from the grips is expected, given that, statistically, some coupons should have their weakest spot near the grips. Secondly, Labs 1 and 7 used a high-speed camera to observe their tests. While the frame rates they used (10000 and 1000 frames per second, respectively) are not nearly high enough to observe the full details, they were often able to detect the failure location. Fig. 8 illustrates a clear case of failure in the gauge section for an arrow coupon. Most of the arrow coupons of this lab failed away from the grips, whereas this was roughly half in the rectangular, tapered, and arrow coupons tested by Lab 1. This supports the consistent results in Fig. 7: if coupons fail away from the grips, then the tabs and gripping method should not be critical. Most sandwich coupons tested by Lab 1 did fail near the grips, which explains why their failure strain values are lower than those obtained by the other labs. We believe this is likely due to the required gripping pressure being too high, which is related to the roughness of the wedge grip surfaces.

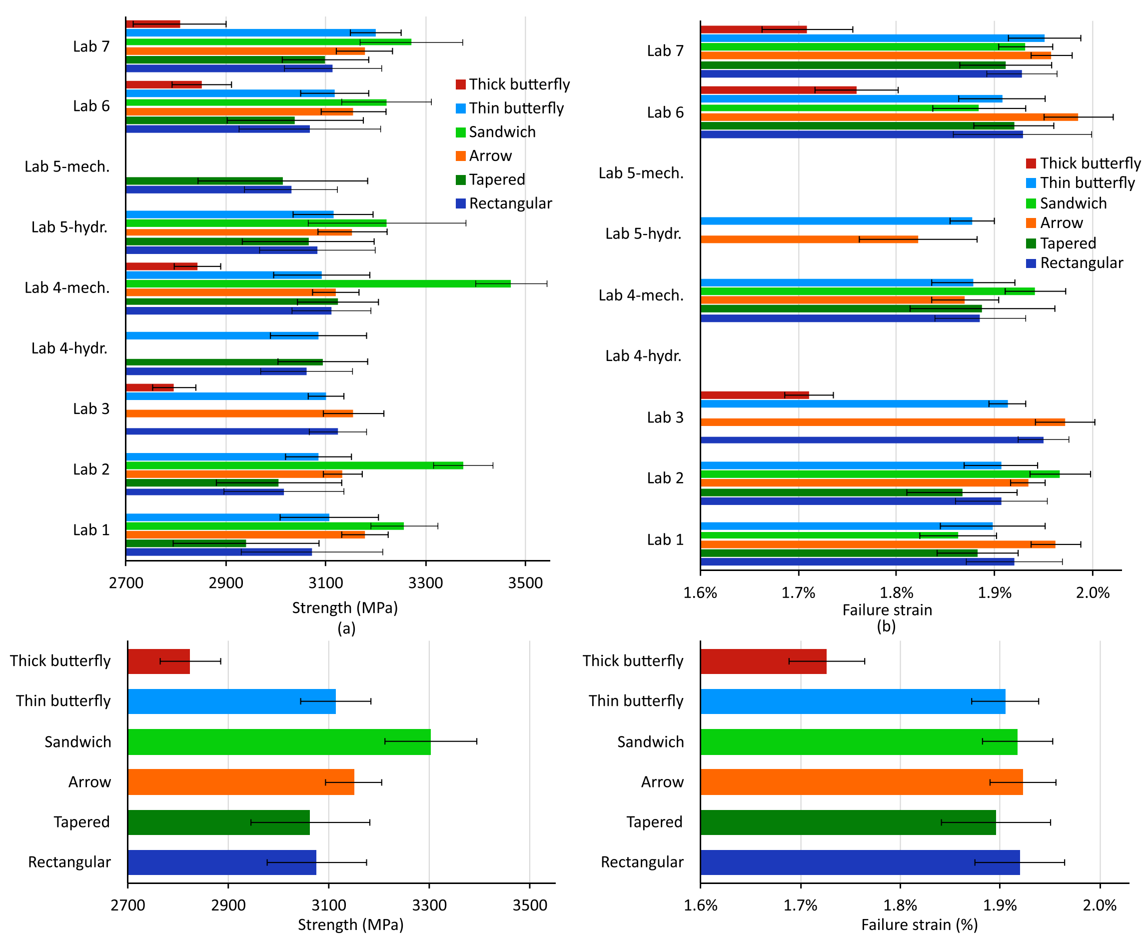

Fig. 7. The average measured (a,c) strength and (b,d) failure strain values and their 95 % confidence intervals for the different labs and coupon designs.

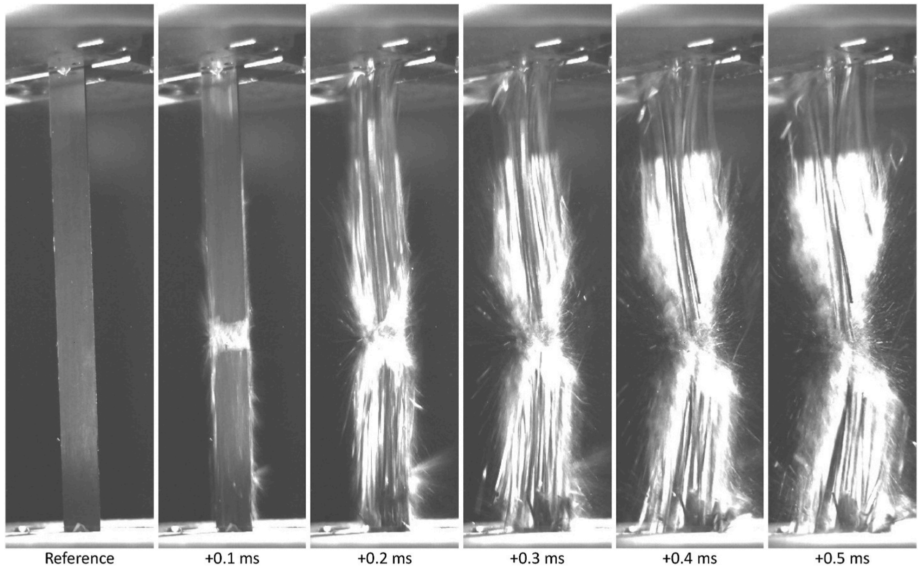

Fig. 8. Six consecutive high-speed camera images of an arrow coupon tested by Lab 1, demonstrating clear failure initiation away from the grips.

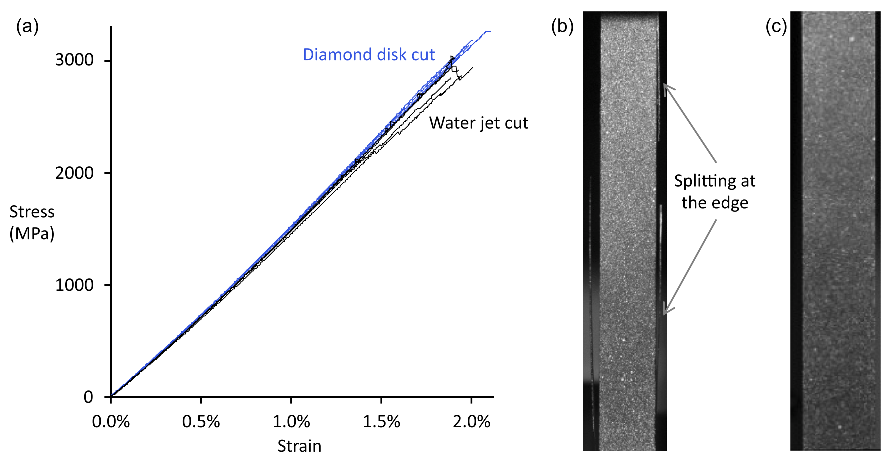

Fig. 9. The difference between coupons cut with diamond disc versus those cut with water jet: (a) stress-strain diagrams, (b) splitting of the water jet-cut coupons, and (c) lack of splitting or minor splitting in diamond disc-cut coupons. These experiments were performed by Lab 1 on the rectangular coupon design.

3.2. Effect of cutting

In preparation for cutting all coupon types, we initially planned to use water jet cutting for all of them. This was because diamond disc cutting was not possible for the butterfly coupons, and machining all the coupons was not an option due to time and personnel constraints. After several attempts to improve the water jet cutting quality, we performed tests to compare the performance of rectangular coupons cut using a diamond disc and water jet. Fig. 9a compares the stress-strain diagrams. The coupons cut by water jet started showing small load drops owing to splitting at the edges (see Fig. 9b) at around 1.5 %, whereas this only appeared very close to the final fracture for coupons cut by diamond disc. The difference in strength was 8.7 % on average, proving that a high-quality cut is vital for reliable results.

The careful coupon preparation also taught us valuable lessons regarding aligning the panel in the diamond disc saw. We had an accurate reference line, but it is still easy to misalign it by 1° during cutting. Breaking a narrow edge piece off along the fibre direction is an excellent way to identify the true fibre orientation. The splits in Fig. 9b are nearly perfectly straight, indicating an excellent alignment and showcasing that splits in this particular case are due to limited cut quality rather than misalignment.

3.3. Effect of testing methodology

In setting up the round-robin programme, we attempted to achieve a consistent testing methodology according to established best practices, where possible, but still gave the participants some freedom. This freedom was mainly intended to reflect the reality and standard testing practices in different labs. This variation also leads to interesting and valuable conclusions.

As illustrated in Table 1, only Lab 3 used a digital height gauge instead of a digital micrometre with a flat tip. This was initially concerning because (1) the coupon was supported over a length of 90 mm, which evens out the variations in the bottom surface, and (2) the height gauge had a ball tip instead of a flat tip, which leads to a more local measurement of thickness. Statistical analysis revealed that the thickness measured with a digital micrometre was 971 ± 11 μm versus 977 ± 7 μm with a digital height gauge (ignoring sandwich and thick butterfly coupons). This difference is small and will not change the conclusions in this round-robin, but it is statistically significant with a p-value of 0.02 %. We believe this effect was small in this case because

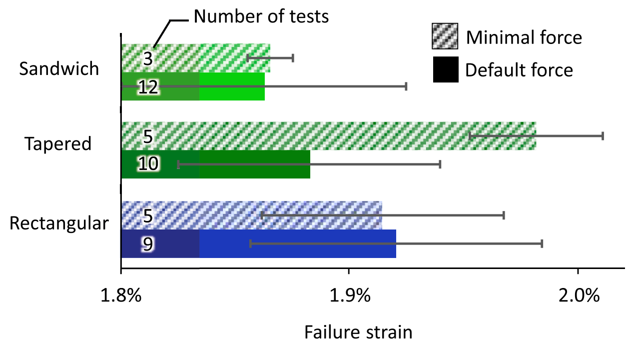

Fig. 10. The effect of gripping force on measured failure strain and standard deviations for three coupon designs tested by Lab 1. The numbers on the bars indicate the number of specimens tested.

both coupon sides were very smooth, and concerns (1) and (2) may cancel out each other.

For all coupons with a nominal thickness of 1 mm (excluding sandwich and thick butterfly coupons), we analysed whether the thickness, modulus, strength, or failure strain for coupons taken from the middle versus the edge of the panel were different. We could not find any such trends, which is indicative of a high test panel quality. This was helped by the fact that the 3900 resin is a no-bleed system. A higher coupon thickness did tend to decrease the modulus by 1.1 GPa on average for every 0.01 mm of thickness, which is a less-than-proportional decrease. The strength decreased by 12 MPa for every 0.01 mm thickness increase, which is also a less-than-proportional decrease. This effect is partially attributed to the fact that a higher coupon thickness is a likely indicator of a lower fibre volume fraction. There may, however, be correlations between fibre volume fractions and local fibre misalignment that are less obvious.

Lab 2 used mechanical grips, whereas other labs used hydraulic grips, and Labs 4 and 5 used both. When the results for rectangular, tapered and arrow coupons are paired based on mechanical versus hydraulic grips, we do not obtain a significant difference in the strength (p-value of 18 %). Lab 2 was the only one that used manual alignment of the grips, and their strength and failure strain results (see Fig. 7) were in line with the other labs. This may indicate that the alignment tools were not critical, but basing this conclusion on just one lab would be premature: it may also be that this lab had good alignment either through chance or careful manual alignment. We also note that a previous study did prove that alignment tools can be important in achieving reliable strength and failure strain values [21], although this study focused on tension-tension fatigue.

For sandwich coupons, Lab 3 reported issues with a too high force in their grips, largely due to the excessive grip capacity and weight (see Table 1). Therefore, all but one of their sandwich coupons failed near the grips, and the measured failure strain and strength values were lower than those of other coupons and labs. This is why their strength and failure strain values were not included in Fig. 7. Therefore, we decided to conduct dedicated experiments to assess the effect of gripping force. The effect of gripping force was studied in Lab 1 on three different coupon designs. Fig. 10 depicts the failure strain of three different coupon designs tested at two different gripping forces. The higher gripping force (applied by the plunger) was the default one used in the original tests (as reported in Figs. 6 and 7) and was 106.3 kN for sandwich coupons and 99.2 kN for rectangular and tapered coupons. After trial-and-error, we found that this force could be reduced to 74.5 kN and 70.8 kN, respectively, without causing slippage, which we refer to as "minimal force". The results show no significant effect on the average failure strain for rectangular and sandwich coupons but a strong improvement for the tapered coupons. For all three coupons, the standard deviations are smaller when the minimal force was applied. In tapered coupons, the high gripping force resulted in failure close to the edge of the end tabs or within the tapered region of the end tabs. However, the minimal force enabled around half of the coupons to fail away from the gripped section. Almost all sandwich coupons failed near the grips at both gripping force levels. The reason for having failure near the grips even after minimising the gripping force might be the roughness of the wedge grip. If the wedge grip surface is insufficiently rough, then the minimum force to avoid slippage can still be high. This issue may be more pronounced with the sandwich coupons, as they are three times as thick as the other coupons (apart from thick butterfly) and require higher force to break the coupon. Note that the tapered coupons tested at minimal gripping force display a failure strain that is significantly higher than those tested at the default gripping force. This value is also statistically significantly higher than any other failure strain reported for tapered coupons in Table 2, but this is not true compared to other coupon types.

We deliberately did not impose any particular strain measurement method because we realised that not all labs have the same facilities, and some have habits or preferences. We, therefore, analysed the modulus measurements for the different techniques for all coupons apart from the sandwich ones. The values were 145.6 ± 3.3 GPa, 146.5 ± 3.6 GPa, 148.9 ± 6.2 GPa and 149.3 ± 3.4 GPa for optical extensometer, DIC, mechanical extensometer and strain gauges, respectively. The differences between the two optical methods and the two contact methods are statistically significant, with a p-value of 10^{-11} %. We do not have a clear explanation for these differences, which are up to 2.5 %. Some researchers argue that strain gauges are the most reliable method to measure the modulus. However, we do not observe this in our data: optical extensometer and full-field DIC are just as good as strain gauges in terms of standard deviation on the modulus measurement. Full-field DIC should be more accurate than optical extensometer since it averages strains over a larger area. Although that is not the case in our data, we do observe a relatively large standard deviation on the modulus measured with a mechanical extensometer. However, we do not draw any conclusion from this observation, as this is linked to only one lab, which faced some difficulties getting the mechanical extensometer to attach well to the coupons.

We also noticed differences in the practical difficulties with the different strain measurement methods. The participants using strain gauges had a significantly higher number of tests that did not yield a reliable failure strain value. While we had 416 successful strength measurements, we only had 316 successful strain measurements. This "success rate" of 76 % was reduced to 71 % for butterfly coupons versus 79 % for all others. The success rate for strain gauge-based measurements was 74 %, which is in line with the average. However, many strain gauge-based experiments also had issues with the strength measurement, which yields a misleading impression of a high success rate. We believe the issue with strain gauge measurements is that splitting at the edge or the surface can disrupt the contact between the strain gauge and the specimen. The sandwich coupons were the most reliable design for measuring the failure strain, with a success rate of 94 % regardless of the strain measurement method. The sandwich design is also expected to work better for thinner coupons, as the relatively thick coupons required high gripping forces, which may have contributed to the slightly premature failure of a number of the sandwich coupons. We decided to still keep the 1 mm thickness for consistent stressed volume across as many coupon types as possible. We believe the success of the sandwich coupons in this regard is because (1) they show minimal splits, (2) the splits that do occur mainly happen in the central carbon fibre layer and not on the external glass fibre layer, and (3) the specimens tend to fail away from the grips.

3.4. Effect of data reduction methodology

When collecting the initial stress-strain data from the participants, we realised that there are different ways to calculate the modulus from

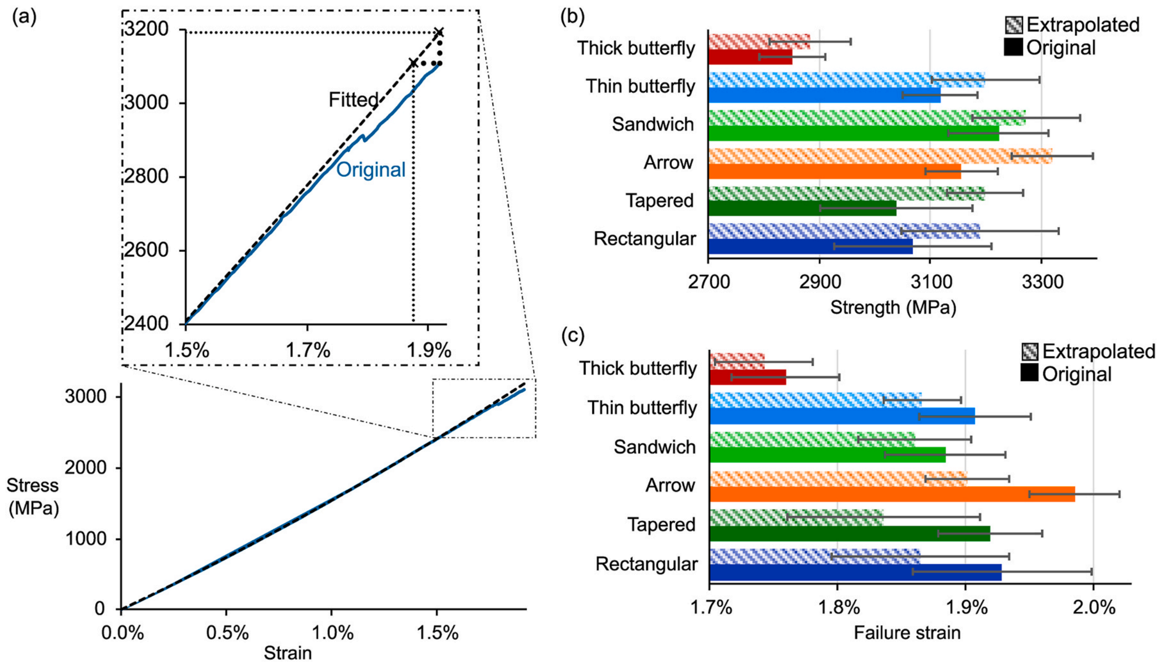

Fig. 11. Extrapolation of a fitted line to obtain strength and failure strain values: (a) an example stress-strain diagram with its fit for a rectangular specimen tested by lab 6, (b) the effect on strength values, and (c) the effect on failure strain values. All these values are based on the results of Lab 6.

the initial section of the diagram. However, there are also different ways to shift the diagram to the origin before extracting the modulus. Therefore, we attempted three different options:

- Method 1: Horizontally shifting so the straight line fitted on all data points between 0.1 % and 0.3 % strain extrapolates through the origin and using the slope of that line.
- Method 2: Horizontally shifting so the straight line fitted on all data points between 0.05 % and 0.25 % strain extrapolates through the origin and using the slope of that line.
- Method 3: Horizontally shifting so the line between the individual data points at 0.1 % and 0.3 % strain extrapolates through the origin and using the slope of that line.

Method 1 was our default. Method 2 aligns with the ISO standard but uses a lower strain interval. Method 3 aligns with the ASTM standard. The resulting modulus and standard deviation for all rectangular coupons were 146.7 $\pm$ 3.3 GPa, 145.0 $\pm$ 3.2 GPa, and 146.8 $\pm$ 3.4 GPa. This reveals that methods 1 and 3 are almost identical, even in terms of standard deviation. Method 2 results in a 1.2 % lower average, which can be attributed to the stiffening of the carbon fibres with applied strain. The measured stiffening corresponds to 24 % for every 1 % strain applied, which matches expectations from the literature [34–36].

We defined failure strain as the strain corresponding to the maximum stress, but we also investigated the effect of alternative definitions for strength and failure strain. Kumar et al. [16] proposed fitting a second-order polynomial to the data and defining the failure strain based on the strain at which this fitted line reached the maximum stress. We also analysed the opposite case, where we defined the strength based on the stress at which the fitted line reached the failure strain. The dotted lines in Fig. 11a illustrate both cases. All our fits were performed up to a strain of 1.5 %, apart from a few cases where we stopped prior to the first small stress drops before this strain level.

Fig. 11b and c illustrate that the extrapolated definition increases the strength by 30–160 MPa, whereas it decreases the failure strain by 0.02–0.08 %. Whether the extrapolated values are better than the regular ones depends on the origin of the discrepancy. If splits occur, then the effective cross-section is reduced, whereas the stress calculation is still based on the original cross-section. The extrapolated strength may be the appropriate value in such cases, but the strain measurement should remain accurate. The splits for butterfly coupons do not necessarily reduce the cross-section but may increase coupon compliance outside of the gauge section. However, the load and strain measurement should remain accurate in that case. This is likely why the differences between fitted and extrapolated values seem smaller for the butterfly coupons. This difference is also small for sandwich coupons, as this coupon design displays minimal or no splitting. The correct definition depends on the origin of the load drops, which may be difficult to identify in practice. Therefore, we recommend optimising the coupon preparation and testing procedure so these load drops are minimised.

4. Recommendations

Although the careful coupon preparation minimised the differences between the labs and the designs, we can still make valuable and novel recommendations related to the coupon designs:

- The non-standardised coupons (arrow, sandwich and thin butterfly) achieved high failure strain and strength values with limited scatter. The standardised rectangular and tapered coupons were almost equally good in this regard.
- The rectangular coupons are the easiest to manufacture. Arrow tabs are also easy to manufacture, but tapered tabs are already more challenging, as they either require chamfering rectangular tabs or directly laminating the tabs in the layup (as was done here). Sandwich coupons require extra lamination procedures. Butterfly coupons could be water jet cut in principle, but we would recommend computer-numerical controlled milling to achieve the best edge quality. The required devices with high rotation speeds are not available in most labs.
- Sandwich coupons yield consistent values for failure strain and a high success rate for failure strain measurements. However, the stress back-calculation may compromise the accuracy of the strength values if the stress-strain data of the monolithic coupon series used for the back-calculation is not consistent enough. Thinner unidirectional carbon/epoxy layers are expected to be less challenging to grip

and test as part of a sandwich coupon as they require significantly lower force to break.
- Thin butterfly coupons performed well, but reliable strain measurements were more difficult due to frequent splitting before the final fracture.
- Thick butterfly coupons underperformed. Their main benefit and purpose lie in testing coupons where a thickness in the order of 1 mm cannot be achieved without machining in the thickness direction, such as for pultruded profiles.

We also make several important recommendations in terms of testing methodology:

- Strain measurement methods that require contact with the coupon (strain gauges and mechanical extensometer) are more likely to face issues measuring the strain until failure. Non-contact methods are therefore recommended if failure strain needs to be measured consistently.
- A high-speed camera is required to reliably identify where the coupons have failed. While failure happens rapidly, a frame rate of 1000/s or higher is enough to gain valuable information.
- Coupons that experienced significant load drops (more than 3 % of their tensile strength) in the stress-strain diagrams or longitudinal splits should be disregarded. If the drops or splits are substantial, a better cut quality or alignment of the cut with the fibre direction may be required.

5. Conclusions

We have reported the results of a round-robin programme for the tensile testing of unidirectional composites. The lab-to-lab variations were larger than the design-to-design variations but overall the results were more consistent than anticipated [10,14,16,37]. This programme therefore established that longitudinal tensile strength can be measured reliably and consistently, establishing a benchmark for future studies into new specimen designs or test methodologies. We attribute this consistency to four factors:

- The panels were high-quality and nearly void-free.
- The 0° fibre orientation in all plies within the laminate was very consistent, so the fibres in all plies were well aligned.
- The cutting of the coupons was very consistent and well-aligned with the fibre direction.
- The coupons were machined (all butterfly coupons) or cut with a diamond disc (all other coupons), which resulted in excellent edge quality.

Meticulous coupon preparation is, therefore, key to testing unidirectional composites accurately. The proposed testing methodology could help to increase the design allowables in the longer term.

In terms of future work, we will engage with standardisation organisations to modify their standards or develop new ones based on the findings of this round-robin programme. It would be useful to confirm some of our conclusions on other types of unidirectional composites, such as thermoplastic composites or composites with poor fibre-matrix bonding. Such composites may be more prone to splitting, making it more difficult to achieve reliable test results. Repeating this exercise for tension-tension fatigue loading could reveal further important aspects, as a recent study indicated that coupon designs that performed well for static tension may not fit for fatigue testing [21]. It would also be useful to study how the 0° ply strength is affected by the neighbouring blocks of off-axis plies, typically present in multidirectional laminates.

CRediT authorship contribution statement

Babak Fazlali: Writing – review & editing, Visualization, Validation, Methodology, Investigation, Formal analysis, Conceptualization. **Christian Breite:** Writing – review & editing, Supervision, Methodology, Investigation, Conceptualization. **Gergely Czél:** Writing – review & editing, Methodology, Investigation, Conceptualization. **Bodo Fiedler:** Writing – review & editing, Supervision, Methodology, Conceptualization. **Dennis Gibhardt:** Writing – review & editing, Methodology, Investigation, Conceptualization. **Masaki Hojo:** Writing – review & editing, Supervision, Methodology, Conceptualization. **Hannes Koerber:** Writing – review & editing, Methodology, Investigation, Conceptualization. **Rajnish Kumar:** Writing – review & editing, Methodology, Investigation, Conceptualization. **María Luisa Velasco:** Writing – review & editing, Methodology, Investigation, Conceptualization. **Ian McEnteggart:** Writing – review & editing, Methodology, Investigation, Conceptualization. **Lars P. Mikkelsen:** Writing – review & editing, Supervision, Methodology, Conceptualization. **Federico Paris:** Writing – review & editing, Supervision, Methodology, Conceptualization. **Ichiro Taketa:** Writing – review & editing, Methodology, Investigation, Conceptualization. **Michael R. Wisnom:** Writing – review & editing, Supervision, Methodology, Conceptualization. **Yentl Swolfs:** Writing – original draft, Visualization, Validation, Supervision, Software, Methodology, Investigation, Formal analysis, Data curation, Conceptualization.

Declaration of competing interest

The authors declare that they have no known competing financial interests or personal relationships that could have appeared to influence the work reported in this paper.

Acknowledgements

CB would like to acknowledge the Research Foundation Flanders for his postdoctoral fellowship COCOMI (1231322N). The work leading to this publication was performed within the framework of HyFiSyn project and has received funding from the European Union's Horizon 2020 research and innovation programme under the Marie Skłodowska-Curie grant agreement No. 765881. GC acknowledges the National Research, Development and Innovation Office (NRDI, Hungary) for support through grant OTKA FK 131882, and the Ministry of Culture and Innovation of Hungary for support from the National Research, Development and Innovation Fund through grant NKKP ADVANCED 149578. He is grateful for support from the Ministry of Culture and Innovation of Hungary under the TKP2021-NVA funding scheme through grant no. TKP-6-6/PALY-2021 and from the Complex Development funding scheme through grant no. 2022–2.1.1-NL-2022-00012 Creation of National Laboratories. GC is also grateful for support through the János Bolyai Research Scholarship of the Hungarian Academy of Sciences and the ÚNKP-23-5-BME-433 New National Excellence Program of the Ministry of Culture and Innovation of Hungary. MH would like to thank ISO/TC61/SC13 on "Composites and reinforcement fibres" for its standardisation activities. The authors would like to acknowledge Sergei B. Sapozhnikov for providing the initial idea for the arrow tabs.

Data availability

All relevant data is available in Zenodo, and this is clearly stated in the manuscript. Link: https://zenodo.org/records/12771361.

References

[1] X. Xu, M.R. Wisnom, K. Chang, S.R. Hallett, Unification of strength scaling between unidirectional, quasi-isotropic, and notched carbon/epoxy laminates, Compos. A. Appl. Sci. Manuf. 90 (Supplement C) (2016) 296–305.
[2] ASTM D3039-14 Standard Test Method for Tensile Properties of Polymer Matrix Composite Materials, ASTM International, Philadelphia, USA, 2014.
[3] ISO 527-1:2019 Plastics - Determination of Tensile Properties - Part 1: General Principles, ISO, Geneva, Switzerland, 2019.

[4] ISO 527-5:2021 Plastics - Determination of Tensile Properties - Part 5: Test Conditions for Unidirectional fibre-reinforced Plastic Composites, ISO, Geneva, Switzerland, 2019.
[5] I. De Baere, W. Van Paepegem, M. Quaresimin, J. Degrieck, On the tension-tension fatigue behaviour of a carbon reinforced thermoplastic part I: limitations of the ASTM D3039/D3479 standard, Polym. Test. 30 (6) (2011) 625–632.
[6] B. Fazlali, S.V. Lomov, Y. Swolfs, Reducing stress concentrations in static and fatigue tensile tests on unidirectional composite materials: a review, Compos. B Eng. (2024) 111215.
[7] J. Yoo, H. Huh, J. Lim, T. Lee, Tensile properties of CFRP manufactured by resin transfer molding considering stacking sequences at various strain rates, J. Compos. Mater. 53 (14) (2019) 2015–2030.
[8] M.M. Tahir, W.-X. Wang, T. Matsubara, A novel tab for tensile testing of unidirectional thermoplastic composites, J. Thermoplast. Compos. Mater. 32 (1) (2019) 37–51.
[9] I. De Baere, W. Van Paepegem, J. Degrieck, On the design of end tabs for quasi-static and fatigue testing of fibre-reinforced composites, Polym. Compos. 30 (4) (2009) 381–390.
[10] M.R. Maheri, An improved method for testing unidirectional FRP composites in tension, Compos. Struct. 33 (1) (1995) 27–34.
[11] J.A. Lavoie, C. Soutis, J. Morton, Apparent strength scaling in continuous fiber composite laminates, Compos. Sci. Technol. 60 (2) (2000) 283–299.
[12] H. Kusano, Y. Aoki, Y. Hirano, Y. Kondo, Y. Nagao, High-speed imaging on static tensile test for unidirectional CFRP, in: H. Kleine, M.P.B. Guillen (Eds.), 28th International Congress on High-Speed Imaging and Photonics, vol 7126, 2009.
[13] G. Czél, M. Jalalvand, M.R. Wisnom, Hybrid specimens eliminating stress concentrations in tensile and compressive testing of unidirectional composites, Compos. A Appl. Sci. Manuf. 91 (2016) 436–447.
[14] B. Fazlali, S. Upadhyay, S. Ashokbhai Ashodia, F. Mesquita, S.V. Lomov, V. Carvelli, et al., Specimen designs for accurate tensile testing of unidirectional composite laminates, Compos. A Appl. Sci. Manuf. 175 (2023) 107799.
[15] M.R. Wisnom, G. Czél, Y. Swolfs, M. Jalalvand, L. Gorbatikh, I. Verpoest, Hybrid effects in thin ply carbon/glass unidirectional laminates: accurate experimental determination and prediction, Compos. A Appl. Sci. Manuf. 88 (2016) 131–139.
[16] R. Kumar, L.P. Mikkelsen, H. Lilholt, B. Madsen, Experimental method for tensile testing of unidirectional carbon fibre composites using improved specimen type and data analysis, Materials 14 (14) (2021) 3939.
[17] G. Czél, Development of sandwich test coupons with continuous protective layers for accurate determination of the tensile failure strain of unidirectional carbon fibre reinforced composites, Compos. A Appl. Sci. Manuf. 187 (2024) 108440.
[18] S. Korkiakoski, P. Brøndsted, E. Sarlin, O. Saarela, Influence of specimen type and reinforcement on measured tension–tension fatigue life of unidirectional GFRP laminates, Int. J. Fatig. 85 (2016) 114–129.
[19] J. Zangenberg, *The Effects of Fibre Architecture on Fatigue Life-Time of Composite Materials* Phd Thesis, Technical University of Denmark, 2013.
[20] I. De Baere, W. Van Paepegem, C. Hochard, J. Degrieck, On the tension-tension fatigue behaviour of a carbon reinforced thermoplastic part II: evaluation of a dumbbell-shaped specimen, Polym. Test. 30 (6) (2011) 663–672.
[21] B. Fazlali, S.V. Lomov, Y. Swolfs, Concerns in tension-tension fatigue testing of unidirectional composites: specimen design and test setup, Compos. B Eng. 272 (2024) 111213.
[22] F. Pierron, A. Vautrin, The 10 ° off-axis tensile test: a critical approach, Compos. Sci. Technol. 56 (4) (1996) 483–488.
[23] C.T. Sun, I. Chung, An oblique end-tab design for testing off-axis composite specimens, Composites 24 (8) (1993) 619–623.
[24] M.R. Wisnom, J.W. Atkinson, Reduction in tensile and flexural strength of unidirectional glass fibre-epoxy with increasing specimen size, Compos. Struct. 38 (1) (1997) 405–411.
[25] M.R. Wisnom, B. Khan, S.R. Hallett, Size effects in unnotched tensile strength of unidirectional and quasi-isotropic carbon/epoxy composites, Compos. Struct. 84 (1) (2008) 21–28.
[26] T. Gordon, X. Xu, L. Kawashita, M.R. Wisnom, S.R. Hallett, B.C. Kim, Delamination suppression in tapered unidirectional laminates with multiple ply drops using a tape scarfing technique, Compos. A Appl. Sci. Manuf. 150 (2021) 106627.
[27] T. Gordon, X. Xu, M.R. Wisnom, B.C. Kim, Novel tape termination method for automated fibre placement: cutting characteristics and delamination suppression, Compos. A Appl. Sci. Manuf. 137 (2020) 106023.
[28] ASTM D5467-10 - Standard Test Method for Compressive Properties of Unidirectional Polymer Matrix Using a Sandwich Beam, ASTM International, Philadelphia, USA, 2010.
[29] Dataset of the round-robin programme for longitudinal tensile testing. https://zenodo.org/records/12771361, 2024.
[30] I. Straumit, S.V. Lomov, M. Wevers, Quantification of the internal structure and automatic generation of voxel models of textile composites from X-ray computed tomography data, Compos. A Appl. Sci. Manuf. 69 (2015) 150–158.
[31] R. Kumar, B. Madsen, H. Lilholt, L.P. Mikkelsen, Influence of test specimen geometry on probability of failure of composites based on weibull weakest link theory, Materials 15 (11) (2022).
[32] X. Zhang, Y. Shi, Z.-X. Li, Experimental study on the tensile behavior of unidirectional and plain weave CFRP laminates under different strain rates, Compos. B Eng. 164 (2019) 524–536.
[33] S.T.S. Al-Hassani, A.S. Kaddour, Strain rate effects on GRP, KRP and CFRP composite laminates, Key Eng. Mater. 141-143 (1997) 427–452.
[34] F. Mesquita, S. Bucknell, D. Leray, S.V. Lomov, Y. Swolfs, Single carbon and glass fibre properties characterised using large data sets obtained through automated single fibre tensile testing, Compos. A Appl. Sci. Manuf. 145 (2021) 106389.
[35] G.J. Curtis, J.M. Milne, W.N. Reynolds, Non-Hookean behaviour of strong carbon fibres, Nature 220 (5171) (1968) 1024–1025.
[36] M. Kant, D. Penumadu, Dynamic mechanical characterization for nonlinear behavior of single carbon fibers, Compos. A Appl. Sci. Manuf. 66 (2014) 201–208.
[37] T. Matsuo, M. Hojo, K. Kageyama, Influence of gripping method on tensile properties of unidirectional thermoplastic CFRP – round-robin activity for international standardization in Japan, J. Compos. Mater. 53 (2019) 4161–4171.